Theoretical and Electrochemical Studies of *Cuminum Cyminum* (Jeera) extract as Green Corrosion Inhibitor for Mild Steel in Hydrochloric Acid Solution

Ambrish Singh[1], Eno. E. Ebenso[2], M. A. Quraishi[1,]*

[1] Department of Applied Chemistry, Institute of Technology, Banaras Hindu University, Varanasi 221 005 (India)
[2] Department of Chemistry, North West University (Mafikeng Campus), Mmabatho, 2735, South Africa
[*]E-mail: maquraishi.apc@itbhu.ac.in

The effect of seed extract of Jeera (*Cuminum Cyminum*) was investigated by gravimetric, potentiodynamic polarization, electrochemical impedance spectroscopy. Polarization results revealed that the extract acted as mixed type inhibitor. It exhibited 93% IE at 300 ppm. The R_{ct} values of electrochemical impedance spectroscopy, R_p values of Linear Polarization and i_{corr} values of Tafel polarization were in good agreement with weight loss values. Langmuir adsorption isotherm was followed by the inhibitor. UV-Visible spectroscopy also confirmed the complex formation between the inhibitor and the mild steel surface. The low value of energy gap (ΔE) further provided support for high efficiency of the extract.

1. INTRODUCTION

Acid solutions are mostly used in the industries for removal of rusts. Use of inhibitors is one of the common methods in industries for protection of metallic corrosion. The known hazardous effect of most synthetic corrosion inhibitors has motivated scientists to use natural products as corrosion inhibitors as they are inexpensive, readily available and renewable sources of materials, environmentally friendly and ecologically acceptable.

Compounds that contain π-bonds generally exhibit good inhibitive properties by supplying electrons via the heteroatoms (N, S or O). Several works on plant extracts as green corrosion inhibitors

have been done [1-11]. Jeera seeds are used in the cuisines of many different cultures, in both whole and ground form. It helps to add an earthy and warming feeling to cooking; making it a staple in certain stews and soups, as well as curries and chili [12, 13]. The main phytoconstituent of Jeera seeds is cuminaldehyde (Figure 1). It is likely to impart good corrosion inhibition activity due to presence of aromatic ring, aldehyde and isopropyl groups as substituents. Survey of literature reveals that no work has been done on Jeera extract as corrosion inhibitors.

The gravimetric and electrochemical techniques were used to study the seed extract. Several isotherms were tested for their relevance to describe the adsorption behaviour of the compounds studied. The effect of temperature on the corrosion behaviour of steel in the absence and presence of the seed extract was also studied.
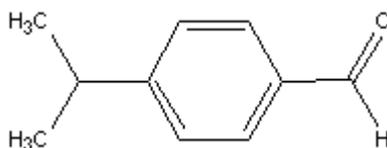
Figure 1. Structure of Cuminaldehyde

2. EXPERIMENTAL

2.1 Inhibitor

Stock solutions of Jeera (*Cuminum Cyminum*) dried seed powder (10 g) was soaked in double distilled water (500 mL) and refluxed for 5 h. The aqueous solution was filtered and concentrated to 100 mL. This extract was used to study the corrosion inhibition properties. Corrosion tests were performed on a mild steel of the following percentage composition: Fe 99.30%, C 0.076%, Si 0.026%, Mn 0.192%, P 0.012%, Cr 0.050%, Ni 0.050%, Al 0.023%, and Cu 0.135%. Prior to all measurements, the mild steel specimens were abraded successively with silicon carbide paper from 600 to 1200 grades. The specimens were washed thoroughly with double distilled water, degreased with acetone and finally dried in hot air blower. And then, the specimens were placed in the desiccator for backup. The aggressive solution of 1 M HCl was prepared by dilution of analytical grade HCl (37%) with double distilled water and all experiments were carried out in unstirred solutions. The rectangular specimens with dimension $2.5 \times 2.0 \times 0.025$ cm^3 were used in weight loss experiments and of size 1.0 $\times$ 1.0 cm^2 (exposed) with a 7.5 cm long stem (isolated with commercially available lacquer) were used for electrochemical measurements.

2.2. Weight loss method

Weight loss measurements were performed on rectangular mild steel samples having size 2.5 $\times$ 2.0 $\times$ 0.025 cm^3 by immersing the mild steel coupons into acid solution (100 mL) in absence and

presence of different concentrations of Jeera (*Cuminum Cyminum*) seed extract. After the elapsed time, the specimen were taken out, washed, dried and weighed accurately. All the tests were conducted in aerated 1 M HCl. All the experiments were performed in triplicate and average values were reported. The inhibition efficiency (η %) and surface coverage (θ) were determined by using following equation;

$$\theta = \frac{w_o - w_i}{w_o} \qquad (1)$$

$$\eta\% = \frac{w_o - w_i}{w_o} \times 100 \qquad (2)$$

where w_i and w_0 are the weight loss values in presence and absence of inhibitor, respectively. The corrosion rate (C_R) of mild steel was calculated using the relation:

$$C_R(\text{mmy}^{-1}) = \frac{87.6 \times w}{AtD} \qquad (3)$$

where w is weight loss of mild steel (mg), A the area of the coupon (cm^2), t is the exposure time (h) and D the density of mild steel (g cm^{-3}) [14].

2.3 Electrochemical impedance spectroscopy

The EIS tests were performed at 308 K in a three electrode assembly. A saturated calomel electrode was used as the reference; a 1 cm^2 platinum foil was used as counter electrode. All potentials are reported versus SCE. Electrochemical impedance spectroscopy measurements (EIS) were performed using a Gamry instrument Potentiostat/Galvanostat with a Gamry framework system based on ESA 400 in a frequency range of 10^{-2} Hz to 10^5 Hz under potentiodynamic conditions, with amplitude of 10 mV peak-to-peak, using AC signal at E_{corr}. Gamry applications include software DC105 for corrosion and EIS300 for EIS measurements, and Echem Analyst version 5.50 software packages for data fitting. The experiments were carried out after 30 min. of immersion in the testing solution (no deaeration, no stirring).

The inhibition efficiency of the inhibitor was calculated from the charge transfer resistance values using the following equation:

$$\mu\% = \frac{R_{ct}^i - R_{ct}^0}{R_{ct}^i} \times 100 \qquad (4)$$

where, R_{ct}^0 and R_{ct}^i are the charge transfer resistance in absence and in presence of inhibitor, respectively.

2.4 Potentiodynamic polarization

The electrochemical behaviour of mild steel sample in inhibited and uninhibited solution was studied by recording anodic and cathodic potentiodynamic polarization curves. Measurements were performed in the 1 M HCl solution containing different concentrations of the tested inhibitor by changing the electrode potential automatically from -250 to +250 mV versus corrosion potential at a scan rate of 1 mV s^{-1}. The linear Tafel segments of anodic and cathodic curves were extrapolated to corrosion potential to obtain corrosion current densities (i_{corr}). From the polarization curves obtained, the corrosion current (i_{corr}) was calculated by curve fitting using the equation:

$$I = i_{corr} \left[\exp\left(\frac{2.3\Delta E}{b_a} \right) - \exp\left(-\frac{2.3\Delta E}{b_c} \right) \right] \tag{5}$$

The inhibition efficiency was evaluated from the measured i_{corr} values using the relationship:

$$\mu\% = \frac{i_{corr}^{0} - i_{corr}^{i}}{i_{corr}^{0}} \times 100 \tag{6}$$

where, i_{corr}^{0} and i_{corr}^{i} are the corrosion current density in absence and presence of inhibitor, respectively.

2.5 Linear polarization measurement

The corrosion behaviour was studied with polarization resistance measurements (R_p) in 1 M HCl solution with and without different concentrations of studied inhibitor. The linear polarization study was carried out from cathodic potential of -20 mV versus OCP to an anodic potential of + 20 mV versus OCP at a scan rate 0.125 mV s^{-1} to study the polarization resistance ($R_{p)}$ and the polarization resistance was evaluated from the slope of curve in the vicinity of corrosion potential. From the evaluated polarization resistance value, the inhibition efficiency was calculated using the relationship:

$$\mu\% = \frac{R_p^{i} - R_p^{0}}{R_p^{i}} \times 100 \tag{7}$$

where, R_p^{0} and R_p^{i} are the polarization resistance in absence and presence of inhibitor, respectively.

2.6. UV-Visible spectroscopy

UV-Visible absorption spectra were measured with Hitachi U-2900 double beam spectrophotometer. The Jeera (*Cuminum Cyminum*) seed extract solution (300 ppm) and the washing

solution obtained after 5 hrs of mild steel immersion at 308 K were subjected to UV-Visible absorption detection.

2.7. Theoretical study

All the calculations were performed with Gaussian 03 for windows. The molecular structures of the neutral species were fully and geometrically optimized using the functional hybrid B3LYP (Becke, three-parameter, Lee-Yang-Parr exchange-correlation function) Density function theory (DFT) formalism with electron basis set 6-31G (*, *) for all atoms. The quantum chemical parameters obtained were EHOMO, ELUMO, EHOMO-LUMO (ΔE), μ, total energy and Mulliken charge on heteroatoms (O).

3. RESULTS AND DISCUSSION

3.1 Electrochemical impedance spectroscopy

Impedance method provides information about the kinetics of the electrode processes and simultaneously about the surface properties of the investigated systems. The shape of impedance gives mechanistic information. Impedance spectra for mild steel in 1 M HCl in absence and presence of different concentrations of seed extract are shown in the form of Nyquist plots (Fig. 2a), Bode-modulus plots (Fig. 2d) and Phase angle plots (Fig. 2e). It followed from Fig. 2a that the impedance of the inhibited mild steel increases with increase in the inhibitor concentration and consequently the inhibition efficiency also increases. A depressed semicircle is mostly referred to as frequency dispersion which could be attributed to different physical phenomena such as roughness and inhomogeneities of the solid surfaces, impurities, grain boundaries and distribution of the surface active sites [15]. The fact that this semicircle cannot be observed after the addition of higher concentration supports our view [16, 17].
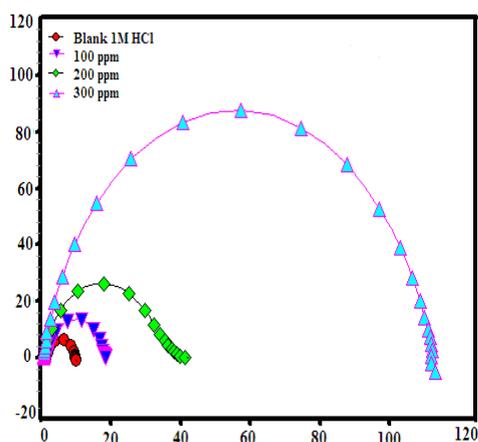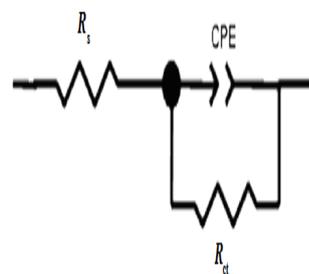
(a)   **(b)**
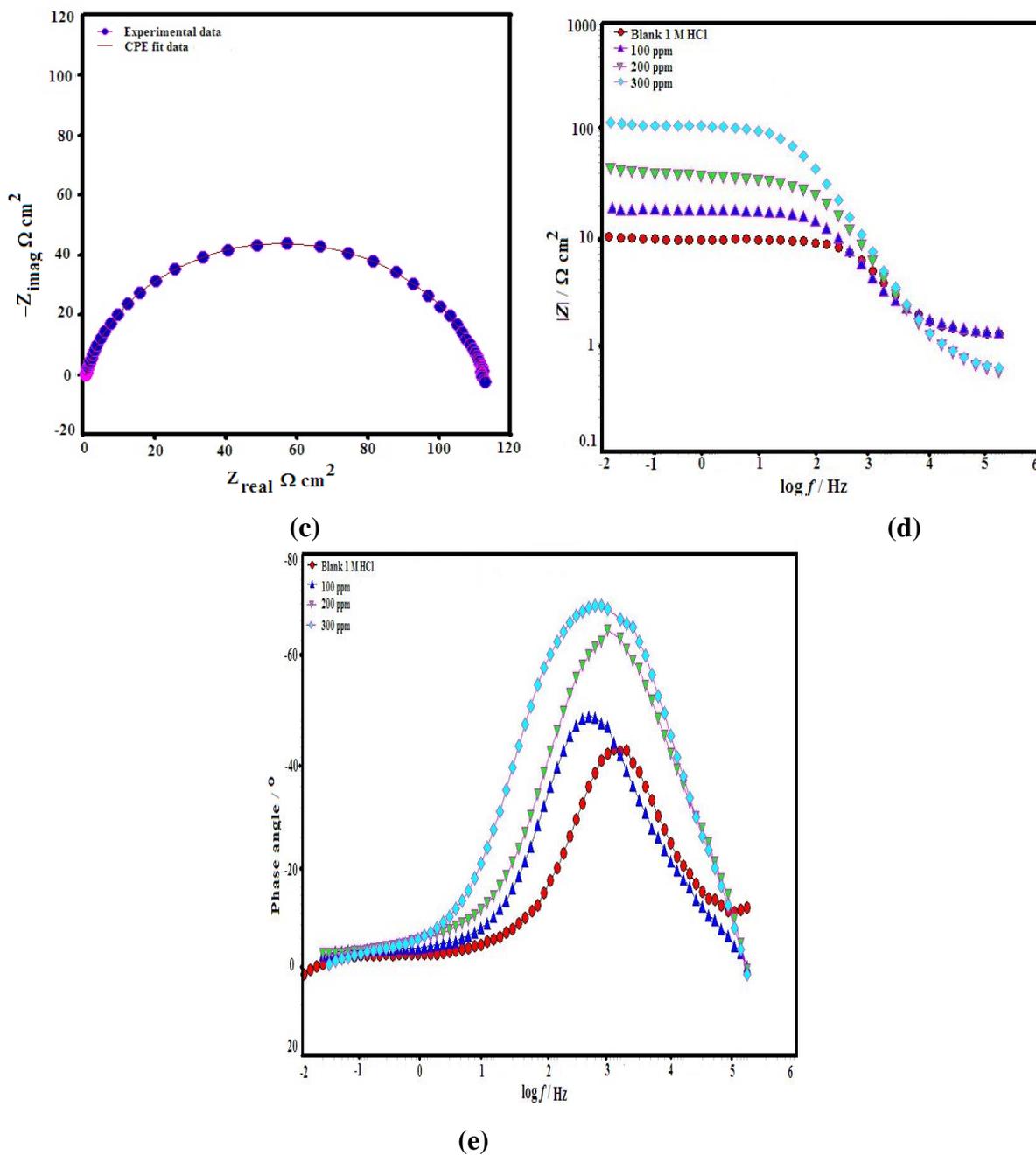
Figure 2. (a) Nyquist plots of mild steel in 1 M HCl in absence and presence of different concentrations of Jeera (*Cuminum Cyminum*) seed extract (b) equivalent circuit used to fit the impedance data (c) Nyquist plot with CPE fit data (d) Bode plot and (e) Phase angle plot

Different corrosion parameters derived from EIS measurements are presented as Table 1. It is shown from Table 1 that R_{ct} of inhibited system increased from 19 Ωcm^2 to 108 Ωcm^2 and double layer capacitance C_{dl} decreased from 47 μFcm^{-2} to 21 μFcm^{-2} with increasing inhibitor concentration. This decrease in C_{dl} results from a decrease in local dielectric constant and/or an increase in the thickness of the double layer, suggested that inhibitor molecules inhibit the iron corrosion by adsorption at the metal/acid interface.

To get more accurate fit of these experimental data, the measured impedance data were analyzed by fitting in to equivalent circuit given in Fig. 2b. Excellent fit with this model was obtained for all experimental data.

Mathematically, amplitude of CPE is given by the relation:

$$Z_{CPE} = Q^{-1}(j\omega)^{-n} \tag{8}$$

where Q is the magnitude of the CPE, j is the imaginary unit, ω is the angular frequency ($\omega = 2\pi f$, the frequency in Hz), and n is the phase shift which gives details about the degree of surface inhomogeneity. When $n = 1$, this is the same equation as that for the impedance of a capacitor, where $Q = C_{dl}$. In fact, when n is close to 1, the CPE resembles a capacitor, but the phase angle is not 90°. It is constant and somewhat less than 90° at all frequencies.

The electrochemical parameters are listed in Table 1. C_{dl} values derived from CPE parameters are listed in Table 1. For providing simple comparison between the capacitive behaviors of different corrosion systems, the values of Q were converted to C_{dl} using the relation [18]:

$$C_{dl} = Q(\omega_{max})^{n-1} \tag{9}$$

where, ω_{max} represents the frequency at which the imaginary component reaches a maximum. It is the frequency at which the real part (Z_r) is midway between the low and high frequency x-axis intercepts.
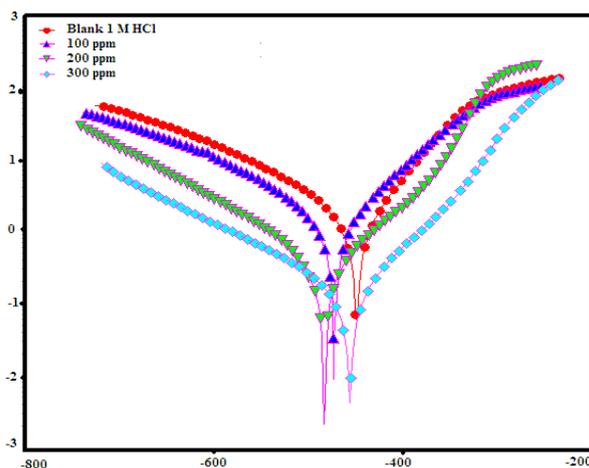
Table 1. Calculated electrochemical parameters for mild steel in absence and presence of different concentrations of Jeera (*Cuminum Cyminum*) seed extract

Inhibitor	Conc. (ppm)	Tafel data					Linear polarization data		EIS data					
		-Ecorr (mv vs. SCE)	icorr (µA cm-2)	βa (mV d-1)	βc (mV d-1)	μ %	Rp (Ω cm2)	μ%	Rs (Ω cm2)	Q (Ω-1 sn cm-2)	n	Rct (Ω cm2)	Cdl (µF cm-2)	μ%
	Blank	446	1540	90	121	-	8	-	1.20	250	0.827	8	69	-
Jeera (*Cuminum Cyminum*) seed extract	100	469	470	101	144	69	38	78	1.31	65	0.817	19	47	57
	200	480	236	77	97	84	69	88	1.47	59	0.854	55	37	85
	300	452	120	59	73	92	119	93	1.72	47	0.869	108	21	93

3.2 Potentiodynamic Polarization

The Tafel polarization curves of mild steel in hydrochloric acid solution, in the absence and presence of different concentrations of Jeera (*Cuminum Cyminum*) seed extract, are presented in Fig. 3 and listed in Table 1. The maximum inhibition efficiency (92%) was obtained at a concentration of 300 ppm.

Addition of the Jeera (*Cuminum Cyminum*) seed extract to acid media affected both the cathodic and anodic parts of the curves. For the inhibited system, if the displacement in E_{corr} value is greater than 85 mV relative to uninhibited system than the inhibitor is classified as cathodic or anodic type. In our case, the maximum displacement of E_{corr} value is 34 mV, hence the Jeera (*Cuminum Cyminum*) seed extract is classified as a mixed-type inhibitor. From the polarization curves it was noted that the curves were shifted toward lower current density region and β_c and β_a values did not showed any significant change [19, 20]. The inhibition efficiency values in the Table 1 showed that the Jeera (*Cuminum Cyminum*) seed extract acted as very effective corrosion inhibitor for mild steel in HCl solution and its capacity of inhibition increased with increase of concentration.

Figure 3. Tafel polarization curves for corrosion of mild steel in 1 M HCl in the absence and presence of different concentrations of Jeera (*Cuminum Cyminum*) seed extract

3.3 Linear polarization measurement

The inhibition efficiencies and polarization resistance parameters are presented in Table 1. The linear polarization values increased from 38 Ω cm^2 to 119 Ω cm^2 resulting in a high inhibition efficiency of 93% at 300 ppm. The results obtained from Tafel polarization and EIS showed good agreement with the results obtained from linear polarization resistance.

3.4 Weight loss measurements

3.4.1 Effect of inhibitor concentration

The effect of inhibitor concentration on inhibition efficiency of steel in 1 M HCl was examined. Maximum inhibition efficiency of 93% was shown at 300 ppm in HCl solution. The values of percentage inhibition efficiency (η%) and corrosion rate (C_R) obtained from weight loss method at different concentrations of Jeera (*Cuminum Cyminum*) seed extract at 308 K are summarized in Table 2.

Table 2. Corrosion rate and Inhibition efficiency values for the corrosion of mild steel in aqueous solution of 1 M HCl in the absence and in the presence of different concentrations of Jeera (*Cuminum Cyminum*) seed extract from weight loss measurements at 308 K

Name of Inhibitor	Conc. of Inhibitor (ppm)	Surface Coverage (θ)	$\eta\%$	C_R (mmy^{-1})
1 M HCl	-	-	-	77
Jeera (*Cuminum Cyminum*) seed extract	50	0.41	41	45
	100	0.60	60	31
	200	0.75	75	19
	300	0.93	93	5

3.4.2 Effect of temperature
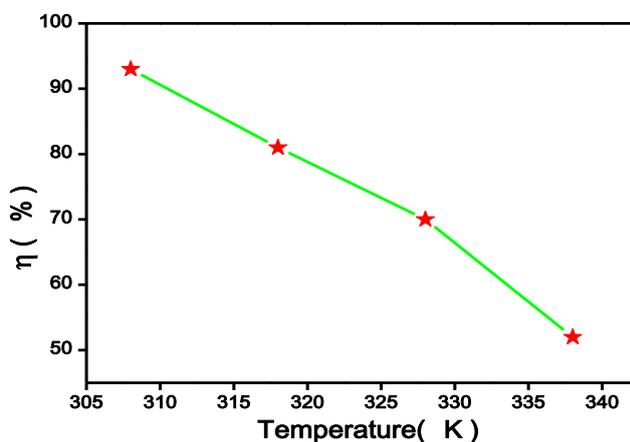
Figure 4. Inhibition efficiency of Jeera (*Cuminum Cyminum*) seed extract at different temperatures

In order to investigate the effect of temperature on the performance of studied inhibitor and to derive thermodynamic activation and adsorption parameters, weight loss studies were performed at four different temperatures as depicted in Figure 4. The inhibition efficiency of Jeera (*Cuminum Cyminum*) seed extract decreases with increasing temperature.

3.4.3 Thermodynamic activation parameters

The dependence of corrosion rate at temperature can be expressed by Arrhenius equation and transition state equation:

$$\log(C_R) = \frac{-E_a}{2.303RT} + \log \lambda \tag{10}$$

$$C_R = \frac{RT}{Nh} \exp\left(\frac{\Delta S^*}{R}\right) \exp\left(-\frac{\Delta H^*}{RT}\right) \tag{11}$$

where E_a apparent activation energy, λ the pre-exponential factor, ΔH^* the apparent enthalpy of activation, ΔS^* the apparent entropy of activation, h Planck's constant and N the Avogadro number.

The apparent activation energy for Jeera (*Cuminum Cyminum*) seed extract is presented in Table 3. As it can be seen from Table 3, the values of activation free energy of Jeera (*Cuminum Cyminum*) seed extract are higher than that of free acid solution. Thus, the corrosion rate of mild steel is mainly controlled by activation parameters.

The linear regreression between log (C_R) vs. $1/T$ (Figure 5a) and log (C_R/T) vs. $1/T$ (Figure 5b) were performed. Straight lines obtained with a slope $(-\Delta E_a/2.303R)$, $(-\Delta H^*/2.303R)$ and an intercept of $\left[\log(R/Nh) + (\Delta S^*/2.303R)\right]$, from which the value of E_a, ΔH^* and ΔS^* were calculated and presented in Table 3.

Table 3. Thermodynamic parameters for the adsorption of Jeera (*Cuminum Cyminum*) seed extract in 1 M HCl on the mild steel

Inhibitor	Conc. (ppm)	E_a (kJ mol^{-1})	$-\Delta G^\circ_{ads}$ (kJ mol^{-1})	ΔH°_{ads} (kJ mol^{-1})	ΔS°_{ads} (J K-1 mol^{-1})	ΔK_{ads} (mol^{-1})
1 M HCl	0	28.77	-	22.17	-136.90	-
Jeera (*Cuminum Cyminum*) seed extract	300	64.21	34	73.24	-52	42,153
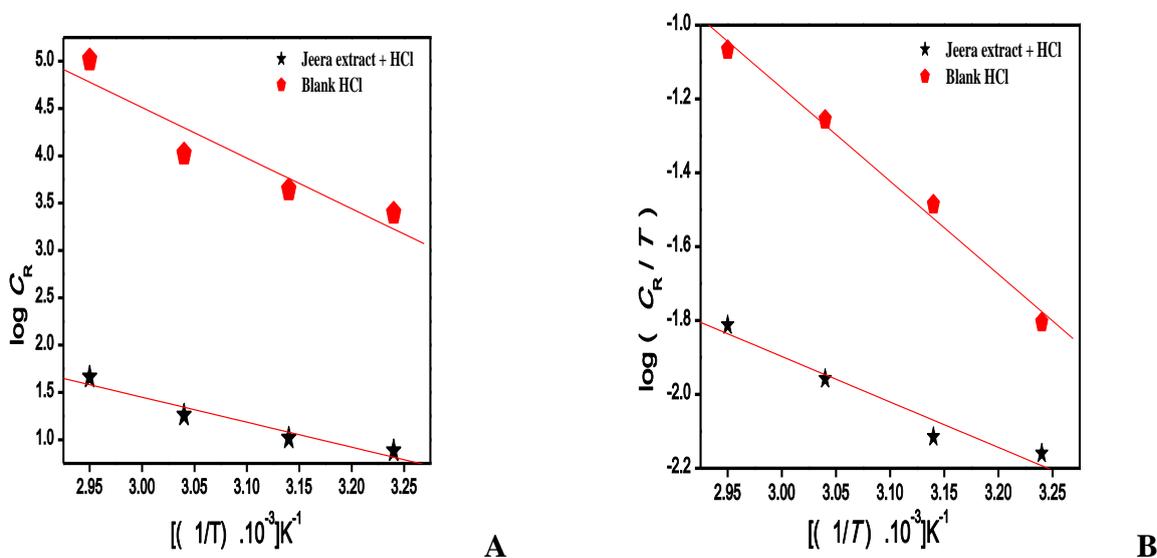
Figure 5. Arrhenius plots for (a) log C_R versus $1/T$ (b) log C_R/T versus $1/T$

3.4.4 Thermodynamic parameters and adsorption isotherm

The efficiency of Jeera (*Cuminum Cyminum*) seed extract molecules as a successful corrosion inhibitor mainly depends on their adsorption ability on the metal surface. To emphasize the nature of adsorption, the adsorption of an organic adsorbate at metal/solution interface can be presented as a substitution adsorption process between the organic molecules in aqueous solution $Org_{(sol)}$, and the water molecules on metallic surface H_2O [21]:

$$Org_{(sol)} + xH_2O_{(ads)} \ \square \ \ Org_{(ads)} + xH_2O_{(sol)} \tag{12}$$
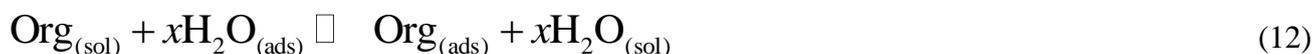
where, x is the size ratio representing the number of water molecules replaced by one molecule of organic adsorbate, $Org_{(sol)}$ and $Org_{(ads)}$ are the organic molecules in the solution and adsorbed on the metal surface, respectively. It is essential to know the mode of adsorption and the adsorption isotherm that can give important information on the interaction of inhibitor and metal surface. Attempts were made to fit surface coverage values determined from weight loss measurements into different adsorption isotherm models (Figure 6a-c). The linear regression coefficient values (R^2) determined from the plotted curves was found to be in the range of 0.99374 for Langmuir, 0.973121 for Temkin and 0.96774 for Frumkin adsorption isotherms at different temperatures studied. According to these results, it can be concluded that the best description of the adsorption behaviour of Jeera (*Cuminum Cyminum*) seed extract can be best explained by Langmuir adsorption isotherm given by equation (13).

Langmuir adsorption isotherm can be expressed by following equation:

$$\frac{C_{(inh)}}{\theta} = \frac{1}{K_{(ads)}} + C_{(inh)} \tag{13}$$

where, C_{inh} is inhibitor concentration and K_{ads} is an equilibrium constant for adsorption-desorption process.

The standard free energy of adsorption of inhibitor (ΔG_{ads}^{o}) and log K_{ads} on mild steel surface can be evaluated with the following equations:

$$\Delta G_{ads}^{o} = -RT \ln(55.5 K_{ads}) \tag{14}$$

$$\ln K_{ads} = \frac{-\Delta H_{ads}^{o}}{RT} + constant \tag{15}$$

The high value of K_{ads} for studied extract indicates stronger adsorption on the mild steel surface in1 M HCl solution. The strong interaction of inhibitor with mild steel surface can be attributed to the presence of O atoms and π-electrons in the inhibitor molecules. The higher K_{ads} value (approximately

>100 M^{-1}), the stronger and more stable adsorbed layer is formed which results in the higher inhibition efficiency [22]. The negative values of standard free energy of adsorption indicated spontaneous adsorption of Jeera (*Cuminum Cyminum*) seed extract on mild steel surface and also strong interaction and stability of the adsorbed layer with the steel surface [23, 24]. Generally, $\Delta G°_{ads}$ values of -20 kJmol^{-1} or higher are associated with an electrostatic interaction between charged molecules and charged metal surface, physisorption; those of -40 kJmol^{-1} or lower involve charge sharing or transfer from the inhibitor molecules to the metal surface to form a coordinate covalent bond, chemisorption. In present case, $\Delta G°_{ads}$ were -34 kJmol^{-1} at 308 K indicating the adsorption of investigated seed extract on mild steel surface is physisorption.


(a)

(b)

(c)
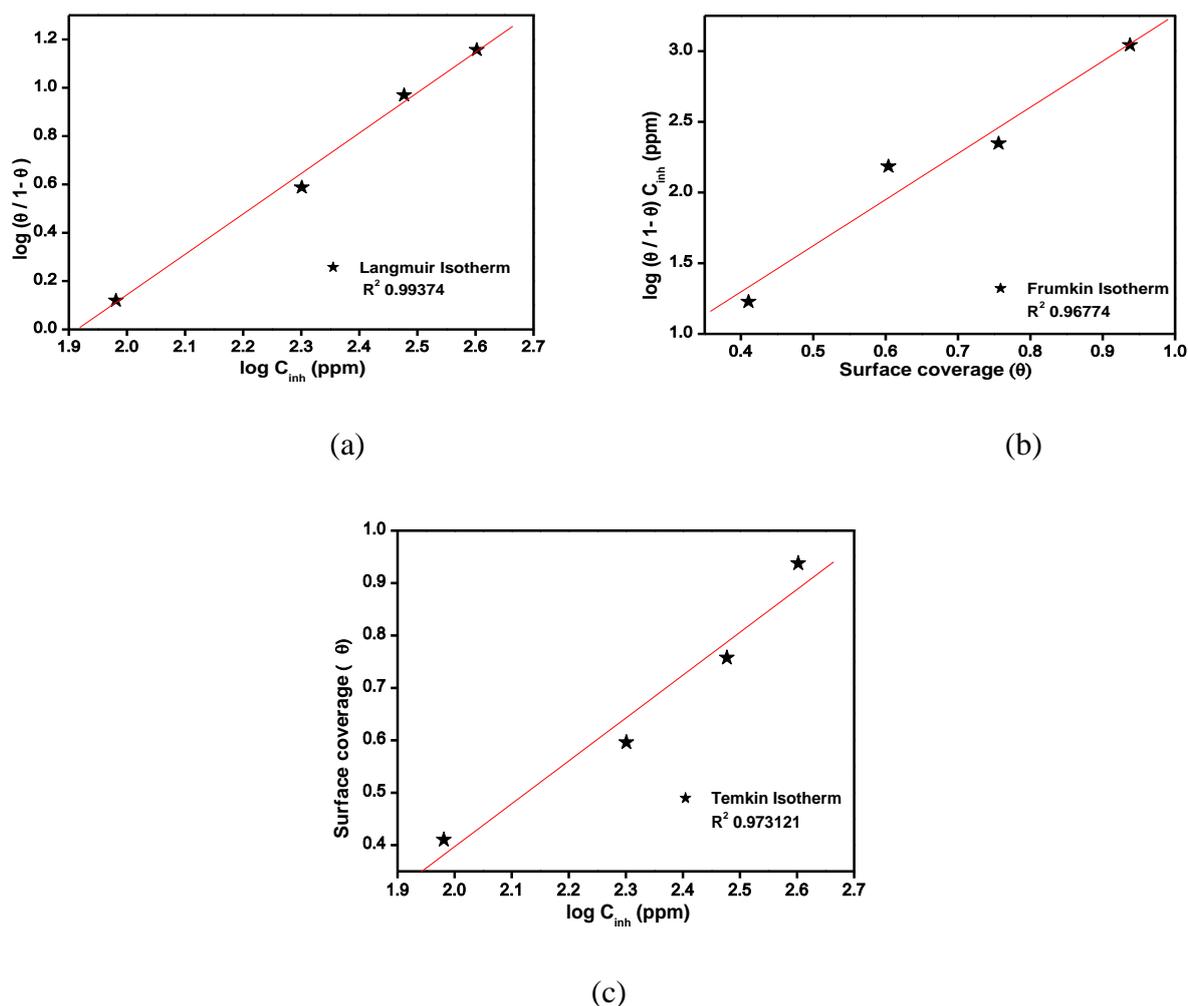
Figure 6. (a) Langmuir (b) Frumkin and (c) Temkin adsorption isotherm plots for the adsorption of Jeera (*Cuminum Cyminum*) seed extract on the surface of mild steel

3.5. UV-Visible Spectroscopy

UV-Visible spectroscopy provides a strong evidence for the formation of a metal complex [25]. We obtained UV-Visible absorption spectra at optimum concentration of Jeera (*Cuminum Cyminum*)

seed extract at 308 K before and after 5 hours immersion of mild steel specimen. The electronic absorption spectrum of Jeera (*Cuminum Cyminum*) seed extract before the mild steel immersion shows two bands in UV-regionas shown in Figure 8. These bands may arise due to π-π^* and n- π^* transitions with a considerable charge transfer character. After 5 hrs immersion of mild steel change in the position of absorption maximum or change in the values of absorbance indicate the formation of a complex between two species in solution. However, there was no any significant change in the shape of the spectra. These experimental findings provide strong evidence for the complex formed between Fe^{2+} and Jeera (*Cuminum Cyminum*) seed extract in 1 M HCl solution. UV-Visible observation confirms the formation of protective film of inhibitor on metal surface.
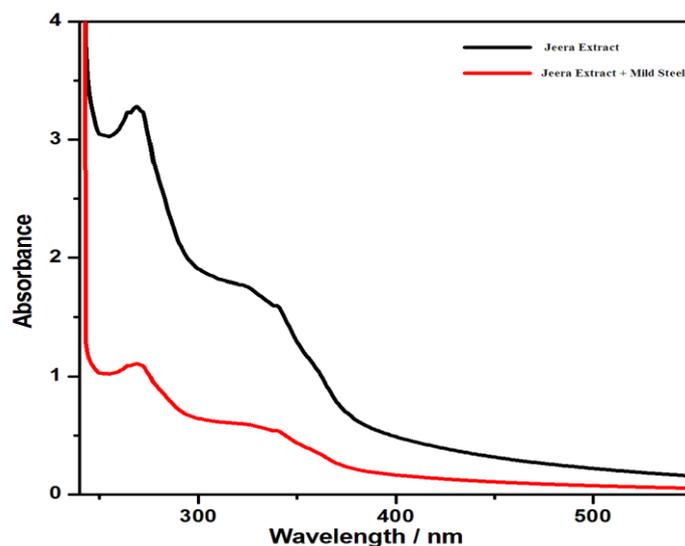

**Figure 7.** UV-Visible spectroscopy with Jeera extract before and after 5 hours immersion of mild steel

3.6. Quantum Chemical Calculations

Quantum chemical calculations were carried out in order to investigate adsorption and inhibition mechanism of studied inhibitor molecules [26]. Figure 8 show full geometry optimization of the inhibitor molecules with Mulliken charges. The Frontier molecular orbital (FMO) density distributions of Cuminaldehyde present in Jeera (*Cuminum Cyminum*) seed extract are shown in Figure 9 (a-b) and total charge density is shown in Figure 10a-b. In order to construct a composite index of an inhibitor molecule it may be important to focus on parameters that directly influence the electronic interaction of the inhibitor molecules with the metal surface. These are mainly: E_{HOMO}, E_{LUMO}, ΔE (E_{LUMO}-E_{HOMO}), and dipole moment μ. The values of calculated quantum chemical parameters such as E_{HOMO}, E_{LUMO}, ΔE (E_{LUMO}-E_{HOMO}), and μ of Cuminaldehyde are listed in Table 4 and Mulliken charges are listed in Table 5.

Frontier orbital theory is useful in predicting adsorption centers of the inhibitor molecules responsible for the interaction with surface metal atoms.
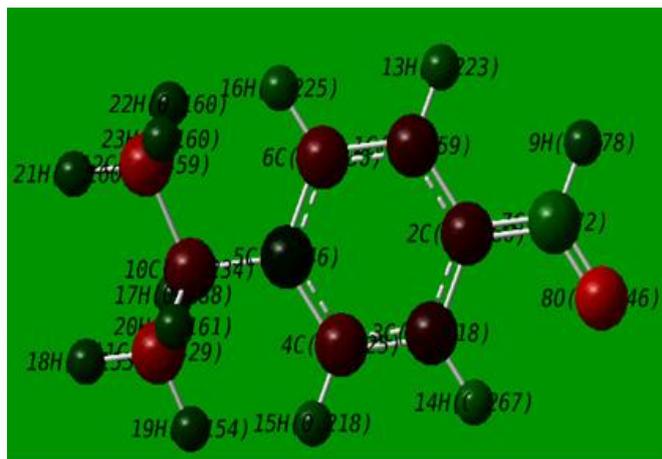
Figure 8. Optimized molecular structure with Mulliken charges of the active constituent (Cuminaldehyde) of Jeera (*Cuminum Cyminum*) seed extract
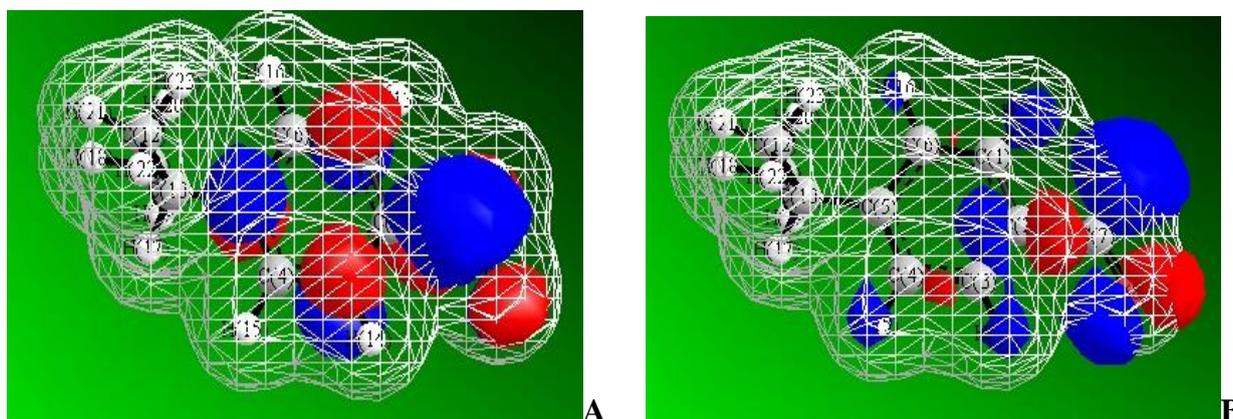
Figure 9. The frontier molecular orbital density distribution of the active constituent (Cuminaldehyde) of Jeera (*Cuminum Cyminum*) seed extract (a) HOMO (b) LUMO)
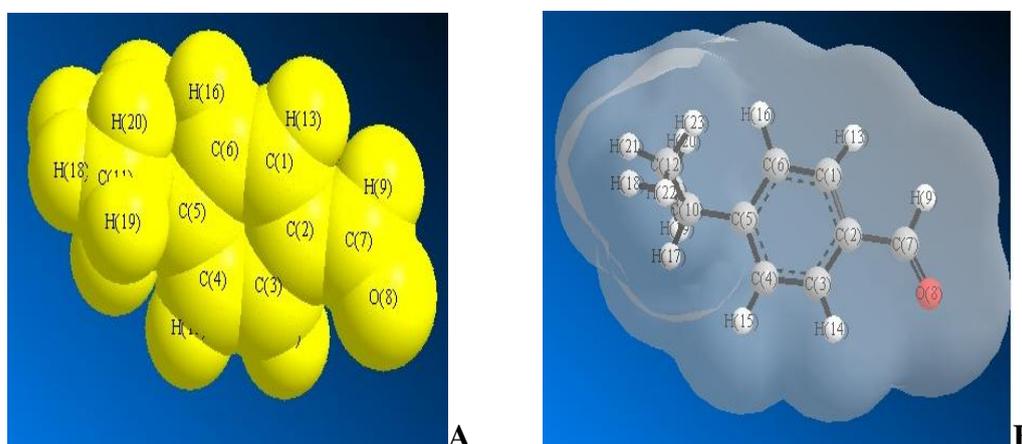
Figure 10. The frontier molecular orbital density distribution of the active constituent (Cuminaldehyde) of Jeera (*Cuminum Cyminum*) seed extracts (a) Total charge density solid view (b) Total charge density transparent view

Terms involving the frontier molecular orbitals could provide dominative contribution, because of the inverse dependence of stabilization energy on orbital energy difference. Lower the value of E_{LUMO}, the more probable; it is that the molecule would accept electrons [27]. As for the values of ΔE (E_{LUMO}-E_{HOMO}) concern; lower values of the energy difference ΔE will cause higher inhibition efficiency because the energy to remove an electron from the last occupied orbital will be low. For the dipole moment (μ), higher values of μ will favor accumulation of the inhibitor in the surface layer [28, 29].

Table 4. Calculated Quantum chemical parameters of studied inhibitor

Quantum Parameters	Cuminaldehyde
HOMO (hartree)	-0.3368
LUMO (hartree)	0.0809
ΔE LUMO-HOMO (hartree)	0.4177
Dipole Moment (μ)	3.2432

Table 5. Calculated Mulliken charges of studied inhibitor

Atoms	Mulliken Charges	Atom Positions
C	0.017	[C(1)]
C	-0.005	[C(2)]
C	0.013	[C(3)]
C	-0.065	[C(4)]
C	0.126	[C(5)]
C	-0.081	[C(6)]
C	0.370	[C(7)]
O	-0.546	[O(8)]
H	-0.012	[H(9)]
C	0.021	[C(10)]
C	-0.117	[C(11)]
C	-0.129	[C(12)]
H	0.023	[H(13)]
H	0.067	[H(14)]
H	0.026	[H(15)]
H	0.032	[H(16)]
H	0.038	[H(17)]
H	0.037	[H(18)]
H	0.039	[H(19)]
H	0.037	[H(20)]
H	0.034	[H(21)]
H	0.040	[H(22)]
H	0.030	[H(23)]

4. MECHANISM OF INHIBITION

Adsorption of Cuminaldehyde in Jeera (*Cuminum Cyminum*) seed extract arises from the donor acceptor interactions between free electron pairs of hetero atoms and π-electrons of multiple bonds, vacant d-orbitals of Fe. In case of adsorption of organic compounds on the metallic surface, planarity of molecules must also be taken in to consideration. The adsorption and inhibition effect of Jeera in 1 M HCl solution can be explained as follows. Jeera molecules might be protonated in the acid solution as

$$\left[C_{10}H_{12}O\right] + xH^+ \rightarrow \left[C_{10}H_{12+x}O\right]^{x+} \qquad\qquad 16$$

The protonated Jeera (*Cuminum Cyminum*) seed extract may adsorb on surface through synergistic effect with Cl$^-$ in hydrochloric acid solution [30]. It is well known fact that the inhibitors which not only offer d electrons but also have unoccupied orbitals, so exhibit a tendency to accept electrons from d-orbital of metal to form stable chelates which are considered as excellent inhibitor [31]. It is not possible to consider a single adsorption mode between inhibitor and metal surface because of the complex nature of adsorption and inhibition of a given inhibitor. It is well known that the steel surface bears positive charge in acid solution; it is difficult for the protonated molecules to approach the positively charged mild steel surface (H$_3$O$^+$/metal interface) due to the electrostatic repulsion. Since chloride ions have a smaller degree of hydration, they could bring excess negative charges in the vicinity of the interface and favor more adsorption of the positively charged inhibitor molecules, the protonated inhibitors adsorb through electrostatic interactions between the positively charged molecules and the negatively charged metal surface. Thus, there is a synergism between adsorbed Cl$^-$ ions and protonated inhibitors. Thus, we can assume that inhibition of mild steel corrosion in 1 M HCl is due to the adsorption of extract constituents on the mild steel surface.

5. CONCLUSIONS

The inhibitor studied has an excellent inhibition effect for the corrosion of mild steel in 1 M HCl. The high inhibition efficiencies of Jeera (*Cuminum Cyminum*) seed extract were attributed to the adherent adsorption of the inhibitor molecules on the mild steel surface. The adsorption of these compounds on the mild steel surface obeyed the Langmuir adsorption isotherm. Potentiodynamic polarization studies revealed that the studied inhibitor is mixed type inhibitor. The results demonstrate that the inhibition by the Jeera (*Cuminum Cyminum*) seed extract were attributable to the adsorption of molecules on mild steel surface. On the other hand, values of the obtained double layer capacitance (C_{dl}) have shown a tendency to decrease, which can result from a decrease in local dielectric constant and/or an increase in thickness of the electrical double layer. Quantum chemical approach is adequately sufficient to predict the structure and molecule suitability to be an inhibitor.

References

1. A. Singh, E.E. Ebenso, M.A. Quraishi, *Int. J. Electrochem. Sci.* 7 (2012) 3409.
2. M.A. Quraishi, A. Singh, V.K. Singh, D.K. Yadav, A.K. Singh, *Mater. Chem Phys.* 122(2010) 114.
3. A. Singh, I. Ahamad, V.K. Singh, M.A. Quraishi, *J. Solid State Electr.* 15 (2011) 1087.
4. A. Singh, V.K. Singh, M.A. Quraishi, *Int. J. Corros.* doi:10.1155/2010/275983.
5. A. Singh, V.K. Singh, M.A. Quraishi, *J. Mater. Environ. Sci.* 1(2010) 162.
6. A. Singh, V.K. Singh, M.A. Quraishi, *Rasayan J. Chem.* 3 (2010) 811.
7. A. Singh, I. Ahamad, V.K. Singh, M.A. Quraishi, *Chem. Engg. Comm.* 199(2012) 63.
8. A. Singh, M.A. Quraishi, *Int. J. Corros.* doi:10.1155/2012/897430.
9. A. Singh, M.A. Quraishi, *J.O.C.P.R.* 4 (2012) 322.
10. A. Singh, M.A. Quraishi, *Res. J. Recent. Sci.* 1 (2012) 57.
11. M.A. Quraishi, D.K. Yadav, I. Ahamad, *The Open Corros. J.* 2 (2009) 56.
12. R. Li, Z.T. Jiang, *Flav. Frag. J.* 19 (2004) 311.
13. L. Wang, *Analyt. Chim. Act.* 647 (2009) 72.
14. M.G. Fontana, . *Corrosion Engineering*, Mcgrawhill, Singapore, 1987, 173.
15. A.M. Badiea, K.N. Mohana, *J. Mater. Eng. Perform.* 18(2009) 1264.
16. M.A. Amin, S.S. Abd El-Rehim, E.E.F. El-Sherbini, R.S. Bayyomi, *Electrochim. Act.* 2007, 52, 3588.
17. M. Kedam,O.R. Mattos, H. Takenouti, *J. Electrochem. Soc.* 128 (1981) 257.
18. C.S. Hsu, F. Mansfeld, F. *Corros.* 57 (2001) 747.
19. M.S. Morad, A.M.K. El-Dean, *Corros. Sci.* 48 (2006) 3398.
20. A. Yurt, A. Balaban, S. Ustun Kandemir, G. Bereket, B. Erk, *Mater. Chem. Phys.* 85(2004) 420.
21. G.K. Gomma, M.H. Wahdan, *Mater. Chem. Phys.* 39 (1994) 142.
22. M. Lagrene, B. Mernari, M. Bouanis, M. Traisnel, F. Bentiss, *Corros. Sci.* 44(2002) 573.
23. M. Hosseini, S.F.L. Mertens, M.R. Arshadi, *Corros. Sci.* 45(2003) 1473.
24. W.H. Li,Q. He, S.T. Zhang, C.L. Pei, B.R. Hou, *J. Appl. Electrochem.* 38 (2008) 289.
25. G. Ji, S.K. Shukla, P. Dwivedi, S. Sundaram, R. Prakash, *Ind. Eng. Chem. Res.* 50 (2011) 11954.
26. Gaussian 03, Revision E.01, Frisch, M.J.; Trucks, G.W.; Schlegel, H.B.; Scuseria, G.E.; Robb, M.A.; Cheeseman, J.R.; Montgomery, Jr. J.A.; Vreven, T.; Kudin, K.N.; Burant, J.C.; Millam, J.M.; Iyengar, S.S.; Tomasi, J.; Barone, V.; Mennucci, B.; Cossi, M.; Scalmani, G.; Rega, N.; Petersson, G.A.; Nakatsuji, H.; Hada, M.; Ehara, M.; Toyota, K.; Fukuda, R.; Hasegawa, J.; Ishida, M.; Nakajima, T.; Honda, Y.; Kitao, O.; Nakai, H.; Klene, M.; Li, X.; Knox, J.E.; Hratchian, H.P.; Cross, J.B.; Bakken, V.; Adamo, C.; Jaramillo, J.; Gomperts, R.; Stratman, R.E.; Yazyev, O.; Austin, A.J.; Cammi, R.; Pomelli, C.; Ochterski, J.W.; Ayala, P.Y.; Morokuma, K.; Voth, G.A.; Salvador, P.; Dannenberg, J.J.; Zakrzewski, V.G.; Dapprich, S.; Daniels, A.D.; Strain, M.C.; Farkas, O.; Malick, D.K.; Rabuck, A.D.; Raghavachari, K.; Foresman, J.B.; Ortiz, J.V.; Cui, Q.; Baboul, A.G.; Clifford, S.; Cioslowski, J.; Stefanov, B.B.; Liu, G.; Liashenko, Piskorz, A. P.; Komaromi, I.; Martin, R.L.; Fox, D.J.; Keith, T.; Al-Laham, M.A.; Peng, C.Y.; Nanayakkara, A.; Challacombe, M.; Gill, P.M.W.; Johnson, B.; Chen, W.; Wong, M.W.; Gonzalez, C.; Pople, J.A.; Gaussian, Inc., Wallingford CT, 2007.
27. I. Ahamad, R. Prasad, M.A. Quraishi, *Corros. Sci.* 52 (2010) 3033.
28. I. Ahamad, R. Prasad, M.A. Quraishi, *J. Solid State Electrochem.* 14 (2010) 2095.
29. D.K. Yadav, M.A. Quraishi, B. Maiti, *Corros. Sci.* 55 (2011) 254.
30. R.S. Goncalves, D.S. Azambuja, A.M. Serpa Lucho, *Corros. Sci.* 44 (2002) 467.
31. G.N. Mu, T.P. Zhao, M. Liu, T. Gu, *Corros.* 52 (1996) 853.